Indirect Tool-Wear Maps for Tool Condition Monitoring in Dry Metal Drilling Operations

A.H. Ammouri, R.F. Hamade

Department of Mechanical Engineering, American University of Beirut, Lebanon

Abstract
To avoid damage to work and/or machine, real-time tool condition monitoring is necessary in automatic and sustainable manufacturing operations. In particular, metal machining with NC machine tools can benefit handsomely from the identification of dull tools in real-time so that they can be replaced. This requirement is especially true in dry (sustainable) drilling operations where heat buildup represents a major challenge.

In this work, quantitative maps of indirect tool-wear of chisel drills undergoing dry machining are charted based only on transducers reporting electrical current measurements from machine (spindle and feed drives) motors. Associated with the maps are qualitative descriptions of the various modes of tool-wear afflicting the drill tools. Based on these tool-wear maps, a novel wear criterion is developed that rely on the % increase in motor (spindle and feed drive motors) RMS current values and is dubbed the Current Rise Index (CRI). For verification, this index is found to positively track the corresponding increase in cutting forces. Utilizing this index, an implementation example is presented in this paper by which a real-time tool monitoring of chisel drills is achieved by inputting the CRI along with the cutting parameters to an Artificial Neural Network (ANN) which yielded good tool condition predictions.

Keywords:
Tool condition monitoring, Current sensors, Dry metal drilling, Sustainability, Tool-wear maps, ANN.

1 INTRODUCTION

Wear of cutting tools is an integral part of the machining process since tool condition affects the dimensional accuracy and surface quality of newly machined surfaces. Although most modes of tool wear are progressive in nature, if not replaced, dull tools are likely to fail in a sudden and catastrophic manner causing damage to both work and machine. Therefore, the successful implementation of tool condition monitoring (TCM) becomes critical to the success of fully automated cutting operations. Over the years, many techniques have been used to monitor and detect tool wear in metal cutting in general and, more relevant to this work, in drilling operations. These involve direct as well as indirect measurements of several types of sensors during drilling that correlate to the condition of the tool. While direct measurements rely on visual and computer vision methods to get dimensional values, indirect measurements include a host of techniques including: sonic and ultrasonic vibration/noise detection [1-4], measurements of cutting forces [5-7], and spindle motor / feed drive current measurements [8-11].

For intelligent prediction of tool wear, the artificial neural network, ANN, method is often used. Typically, the network is trained in the first stage where sensor data is fed to the diagnostics software. Once the software has been 'taught' to distinguish a good (sharp) tool from a partially worn one and from a completely dull one, the diagnostic capabilities of the software become automatic resulting in the real-time correct identification of the drilling tool condition by the software. Such an approach has been utilized in [12] where the root mean square (RMS) value of the spindle motor current was used as input to a multilayer neural network.

In this paper, we utilize sensors to instantly measure RMS current of 1) drilling feed drive motor and 2) spindle motor. Further, we establish tracking between these current measurements with corresponding force measurements and, more importantly, with measured tool-wear at various stages of wear. The resulting wear maps are based on a simple measure, dubbed the 'Current Rise Index (CRI)' and which is derived from the increase in RMS current values.

2 EXPERIMENTAL PROCEDURE

In the performed experiments, 2 brands of 10mm HSS classical twist drills were used: TERA (Tera Autotech Corporation, No. 1 Industrial Park 7 Rd., Tachia, Taichung Hsien, Taiwan, R.O.C.) and IRWIN (Irwin Tools, 92 Grant Street, Wilmington, OH, USA). The drilled material was low carbon steel and the 66-holes pattern shown in Figure 1 was used in all drilling trials.

The following cutting conditions were used:

- Drill starts at a height of 3 mm above the workpiece
- Dry drilling depth of 3 mm to ensure full lip engagement
- Feeds and speeds as in Table 1
- Air (not liquid coolant) was used to cool the tool during the cut and during travel

Cutting parameters in the test matrix are chosen so that cutting speeds range from 40 to 55 m/min (1273 to 1750 RPM) and feeds from 0.03 to 0.2 (mm/rev). The resulting test matrix is shown in Table 1 where for example, test cell C2 corresponds to spindle speed of 1750 RPM and feed of 0.06 mm/rev, respectively.

G. Seliger et al. (eds.), *Advances in Sustainable Manufacturing: Proceedings of the 8th Global Conference on Sustainable Manufacturing*, DOI 10.1007/978-3-642-20183-7_17,

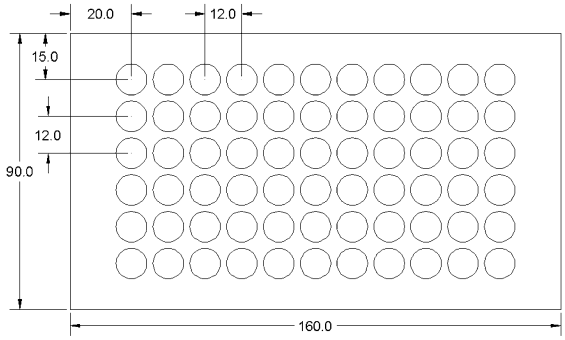

Figure 1: Pattern used in drilling into the low carbon steel

Table 1: Test matrix showing experimental spindle speeds (RPM) and feeds (mm/rev)

		Feed (mm/rev)			
		0.03	0.06	0.1	0.2
Speed (RPM)	1273	A1	A2	A3	A4
	1592	B1	B2	B3	B4
	1750	C1	C2	C3	C4

Current value measurements were carried out by using hall-effect current transducers that were tapped to individual lines of both the spindle motor and the Z-drive motor of a CNC HAAS 5-axis vertical machining center. G-codes were written for each cell in the test matrix. A S22P series current transducer from TAMURA (http://www.tamuracorp.com/clientuploads/pdfs/engineeringdocs/S22PXXXS05.pdf) was used for the spindle motor with a 15A rated current and a LTS6-NP from LEM (http://www.lem.com/hq/en/component/option,com_catalog/task,displaymodel/id,90.37.09.000.0/ was used for the Z-drive motor with a 6A current rating. Both transducers output a 2.5V biased voltage with a 2.5±0.625V full current output voltage.

Signals from the current transducers were acquired by an NI USB-6251 Legacy DAQ device (http://sine.ni.com/nips/cds/view/p/lang/en/nid/209213) into user-friendly LabVIEW software programmed especially for this application. Samples are acquired at a 10K Hz sampling frequency in 2KS batches. The output of the software is raw voltage that represents the cutting cycle current. This raw data is then carefully analyzed to extract the RMS of each cutting trial. Force measurements were collected using Kistler's CompacDyn 3-Component Dynamometer (Type 9254). The Kistler 5070A charge amplifier acquires and amplifies the signal emanating from the dynamometer which is then processed through the Dynamometer's Dynoware data acquisition software (at 1000 Hz).

3 EXPERIMENTAL RESULTS

The results of the experimental study are presented in this Section.

3.1 Flank-wear

As drilling progresses, so do tool wear causing the drill to go from a 'sharp' condition, through a partially worn condition, and ultimately to a dull 'worn out' condition. Catastrophic failures were observed when drilling commenced using dull tools. Wear in drills afflict all regions where metal comes in contact with the drill. However, of the many modes of wear investigated, flank wear, *VB*, is by far the most popular in the metal cutting literature. While many methods exist to quantify flank wear, including taking the average of wear distance at locations along the lip, this work utilizes the maximum *VB*, VB_{max}, at the point where the lip meets the margin and where cutting speeds are largest [13].

Figure 2 shows a TERA twist drill at 3 different stages of progressive wear (a) sharp condition and (b) and (c) at 2 different stages of progressively more worn states of wear with all conditions corresponding to test cell C2. Figure 3 is a typical plot of progressive flank wear of the drill. The three circles on the plot correspond to the 3 stages of wear progression shown in Figure 2.

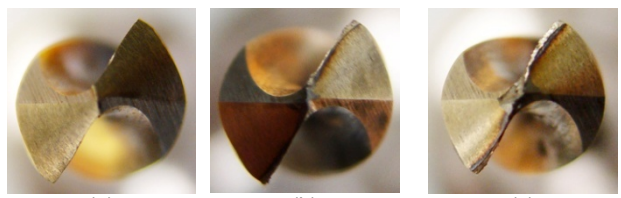

(a) (b) (c)

Figure 2: TERA twist drill shown at (a) sharp condition (b) and (c) at 2 different stages of progressive wear; test case C2.

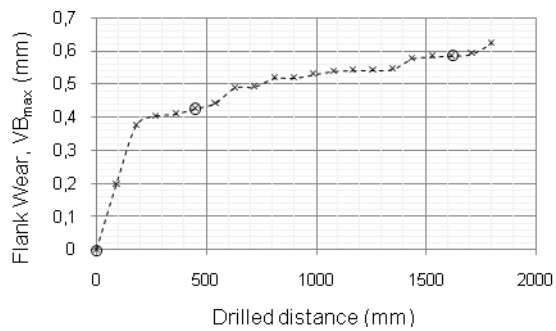

Figure 3: Typical plot of progressive flank-wear of the TERA twist drill; note that circles correspond to images in Figure 2 (test case C2).

3.2 Z-Drive Current

While both torque and thrust force progressively increase as the drill tool undergoes wear [7], thrust force has been found to be more sensitive to drill-wear [14]. To eliminate the usage of the expensive (and machine-tool unnatural) force measurement setup, current measurements of the Z-drive motor line are considered. The LTS6-NP current transducer produces real-time current values with a 400 ns response time. A conditioned calibrated signal of the Z-drive current is shown in Figure 4 superimposed on another signal generated from another drilling test in air (test case B3). The frequency of this particular signal is equal to 3.5 Hz or one full motor cycle = 0.28 s (the value of which depends on the Z-motor driver output for the feed of test case B3 = 0.1 mm/rev). The

shown signal corresponds to a tool with drilling history of 7.524 m. Although the two plots are virtually super imposable during the approach stage, significant deviation is recorded during drill engagement. Note that the reason why less current is needed to drive the motor during the drilling stage as compared with during air-drilling is due to the fact that thrust force acts in an opposite direction to tool motion (and gravity). To get a quantitative value of the current, the RMS of the signal is taken into account throughout this paper. In order to remove the bias due to the current consumed from driving the spindle assembly, the RMS of each drilling cycle is subtracted from the current exerted during the air-drill stage for the same drilling conditions.

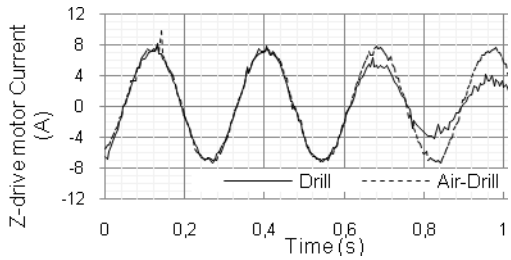

Figure 4: Z-drive motor's true current for a typical signal (one full motor cycle = 0.28 s) generated from an actual drilling test superimposed on another corresponding to an air-drilling test (both for the same parameters: test case B3, drilled distance 7.524 m).

Figure 5 shows the percent increase in measured thrust force values taken over many drilling cycles are found to track fairly accurately that of the percent increase in Z-drive current. Shown in the figure are two superimposed plots of normalized thrust force and Z-drive current over a drilling distance of 1 m (TERA drill; test case C2). Maximum flank wear VB_{max} (mm) is also shown on the secondary axis. The figure indicates that the increase in Z-drive current values is as sensitive as thrust force in tracking flank-wear progression. It can be seen that both sensors (thrust force and current) increase along with progressing tool-wear. The amount of current consumed by the Z-drive motor can be scaled to represent the thrust force.

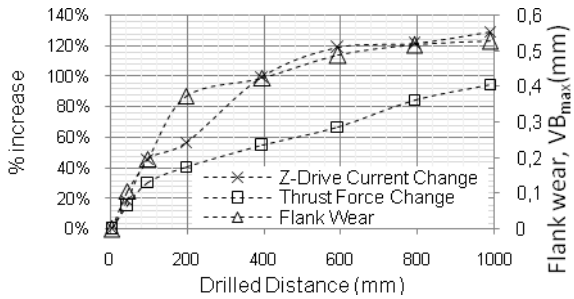

Figure 5: Normalized % change in thrust force and Z-drive current vs. drilled distance for a TERA drill (test case C2).). Progressive flank-wear, VB_{max}, values are also plotted on the secondary axis.

3.3 Spindle-Motor Current

Similar to the Z-drive motor, spindle-motor current values were collected by the S22P transducer at a rate of 10 Ks/s. Figure 6 shows a sample of the collected raw data that corresponds to the same test cell of Figure 4. As wear progresses, the RMS peak value of the spindle-motor current increases given that the motor draws more current to compensate for additional tool-wear.

The effect of drill-wear on the spindle motor current can be observed in Figure 7 which plots the measured progressive VB_{max}, spindle current (RMS), and Z-drive current versus the drilled distance (mm) for a TERA drill (test case C2).

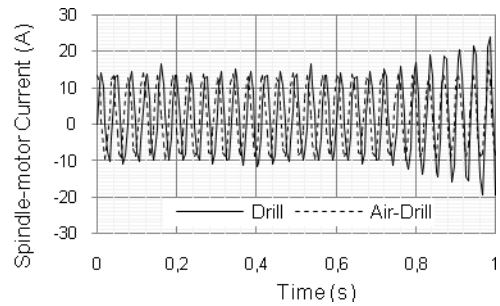

Figure 6: Spindle-motor true current for a typical signal (one full motor cycle = 0.28 s) generated from an actual drilling test superimposed on another corresponding to an air-drilling test (both for the same parameters: test case B3, drilled distance 7.524 m).

3.4 Summary of raw data

For each cell in the test matrix shown in Table 1 a plot that shows the variation of spindle motor current and Z-drive current with the progressive wear is produced. This plot will help in generating the tool-wear maps and the ANN input vector.

Figure 7 is a data summary plot for a TERA drill which shows the increase of the normalized current for Z-drive and spindle motors over drilled distance of 1800 mm (test case C2). Also co-plotted are the maximum flank wear, VB_{max}, values.

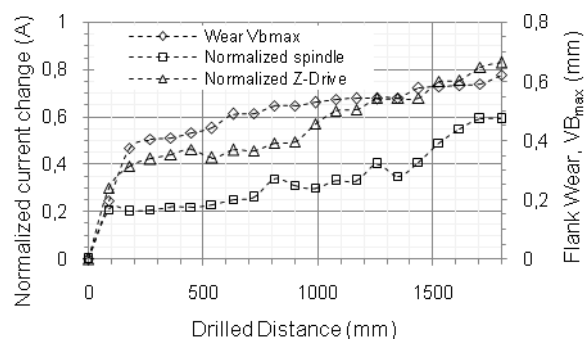

Figure 7: Normalized spindle current (RMS) and Z-drive current vs. drilled distance for a TERA drill (test case C2). Progressive flank-wear, VB_{max}, values are also plotted on the secondary axis.

4 TOOL-WEAR MAPS

A novel representation of progressive tool-wear is presented below based on the acquired data from the current transducer signals. The resulting map is a polar plot based on a measure dubbed here as the Current Rise Index (*CRI*) calculated as the square root of the percent increase in the RMS current values of both transducers. This measure combines both signals in one value that represents the change in current values according to

$$CRI = \sqrt{\left(\Delta I_{Spindle}\right)^2 + \left(\Delta I_{Z-motor}\right)^2} \quad (1)$$

Where:

$\Delta I_{Spindle}$ is the % change in spindle motor current

$\Delta I_{Z-motor}$ is the % change in Z-drive motor current

The percentage change in the current signal is found by subtracting the RMS value of the trial being considered from the air-drill RMS value and dividing the result by the RMS value of the first trial as follows

$$\Delta I_i = \frac{I_i - I_1}{I_1 - I_0} \quad (2)$$

where:

I_i is the RMS value of the test considered

I_0 is the RMS value of the air-drill test

I_1 is the RMS value of the first (wear-free) test

The representation in (2) eliminates the bias of the current signal that comes from the machine dynamics and normalizes the signal such that the first reading is null and the consecutive values are calculated relative to the first trial.

One interesting aspect about *CRI* is revealed by examining (1) which combines 2 complimentary aspects of force generation required for drilling: Z-drive current which is responsible for the feed force action of the drill and spindle current which corresponds to the torque exerted by the spindle. This combination offers wear criteria sensitivity towards both ends of the spectrum where detecting of tool wear affecting either thrust or torque will be possible. It is found in this work that some forms of wear have greater effect on thrust or torque which makes the criteria of practical use in drilling operations irrespective of the specific tool-mode.

Table 2 describes the different ranges of *CRI* and the corresponding tool conditions. For example, a *CRI* value of 1 indicates a 100 percent increase in drilling power-consumption from the starting value. An increase by more than 120 percent means that the tool is dull and should be changed. The values and ranges shown in the table were based on two criteria (1) the drastic increase in power consumption of both motors and (2) the high tool-wear value. Such *CRI* target classifications may equally serve as a measure of wear which lends itself to easy monitoring by human operator, automatic machine tool, or for AI methods such as neural networks as will be shown in Section 5.

Table 2: Wear class criteria, the corresponding CRI values and ANN target value

CRI value			
Min	**Max**	**Tool-Wear Class**	**ANN target**
0	0.29	Sharp – Class 1	1
0.3	0.64	Slightly Worn – Class 2	0.75
0.65	1.19	Workable – Class 3	0.5
1.2	-	Dull – Class 4	0

On a polar wear map, the CRI value and the drilled distance represent the magnitude (ρ) and the angle (θ), respectively, of any point plotted. Figure 8 shows such a tool-wear map corresponding for select cells from the test matrix (Table 1). Both tool brands were tested to show the difference between a low-quality tool and another tool of better quality. A jerk in a wear-map curve indicates a sudden breakage in the tool. The polar wear plot of a desirable tool performance may behave similar to that shown for IRWIN test case B4 where the *CRI* increases smoothly and gradually with low wear rates as the drilling proceeds. Alternately, a bad performance example is the TERA test case B2 where the *CRI* index increased drastically after only a few drills. Although C1 IRWIN (b) and C1 IRWIN (a) are run for the same test case, the jerk seen in he plotted polar curve in C1 IRWIN (a) performance is due to a catastrophic failure in one of the tool flanks.

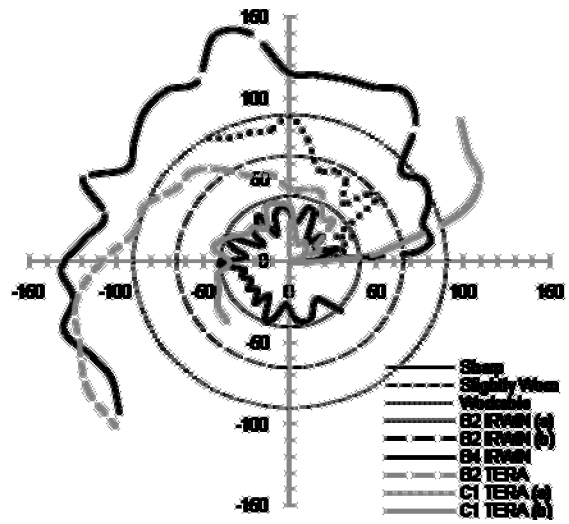

Figure 8: Tool wear maps for select cells of the test matrix performed for drills from both suppliers: TERA and IRWIN.

5 TOOL WEAR PREDICTION WITH ANN

From above, machine tool's motor sensor signals were found to increase as tool wear increased. But the mathematical functional relationship between these signals and tool wear is unclear and is challenging to represent in equation form. In order to combine the signal data from the sensors used and have a functional classification or decision making system, some form of learning or pattern recognition needs to be implemented, in which the machine or program 'learns' how to classify the wear output given the signals inputs. This is done by comparing the values of certain signal inputs to predefined

targets. One solution to such a problem is the use of an artificial neural network (ANN) where a neural network emulates a biological neural system in the sense that in a sort of feedback mechanism or learning, optimizes its neural connections or weights to attain a specified target output. In this work, the dual sensor data is integrated into the ANN software module in MATLAB (where a specific type of networks called multiple-layer-perceptron (MLP) network was implemented). Inputs to the network are:

1. Cutting parameters: spindle speed and feed
2. Number of holes (drilled distance)
3. Main spindle motor current (RMS)
4. Z-drive motor current (RMS)

The only desired output is the tool flank wear. The cutting parameters and sensor features represent the input vector according to Equation (3) and the MLP with one hidden layer and an output layer was trained to output the current state or condition of the tool according to Table 2:

$$p = \left(D, N, f, \Delta I_{spindle}, \Delta I_{z-motor}\right) \quad (3)$$

where

D is the drilled distance

N is the rotational speed

f is the feed rate

This novel wear criterion does not use wear distance as of itself to describe tool condition deterioration but rather uses indirect indicators derived from the machine tool's actual motors current consumption.

MLP network was implemented and tested with 20 neurons in the hidden layer and the 4 'wear class output' criteria. This network used scaled conjugate gradient back-propagation as its learning algorithm. After training this network with data samples corresponding to the experiments in Table 1, the network was given 40 sample inputs and the network outputs were compared to the target classes. The resulting 'confusion (or matching) matrix' which is defined as one that compares the 'wear output class' with 'target class' is shown in Table 3. The results indicate good agreement with the experimental assessment of the state of wear for the cases used to test the network. Out of the 40 test samples, only 3 misclassifications were noticed which corresponds to 92.5% prediction accuracy.

6 SUMMARY

A novel criterion, dubbed the Current Rise Index (CRI), based only on the % increase in the machine tool's spindle and feed motors RMS current values due to tool wear has been presented. Based on this criterion, novel tool wear maps have been introduced which lend themselves to easy decision making by machine operators' visual inspection and monitoring. These maps were demonstrated to be equally useful for automated decision making purposes where artificial neural networks, ANN, were able to make correct determinations about tool (here, drill) condition.

Table 3: Confusion matrix of a test run of 40 samples

Output Class \ Target Class	1	2	3	4	
1	9 22.5%	0 0.0%	0 0.0%	0 0.0%	100% 0.0%
2	1 0.25%	10 25%	2 0.5%	0 0.0%	76.9% 23.1%
3	0 0.0%	0 0.0%	8 20%	0 0.0%	100% 0.0%
4	0 0.0%	0 0.0%	0 0.0%	10 25%	100% 0.0%
	90% 10%	100% 0.0%	80% 20%	100% 0.0%	92.5% 7.5%

7 ACKNOWLEDGEMENTS

The authors wish to acknowledge the financial support of the University Research Board (URB) of the American University of Beirut. The first author also gratefully acknowledges the support of Consolidated Contractors Company through the CCC Doctoral Fellowship in Manufacturing.

8 REFERENCES

[1] M. Mathew, P. Pai, P., and L. Rocha, 2008, An Effective sensor for tool wear monitoring in face milling: acoustic emission. Sadhana, 33/3.

[2] U. Schehl, 1991, Werkzeuguberwachung mit Acoustic-Emission beimDrehen, Fra¨sen und Bohren, Aachen.

[3] S.R. Hayashi, C.E. Thomas, D.G. Wildes, 1998, Tool break detection by monitoring ultrasonic vibrations, Annals of the CIRP 37 (1) 61–64.

[4] K. Kutzner, U. Schehl, 1998, Werkzeuguberwachung von Bohrernkleinen Durchmessers mit Korperschall-sensoren, Industrie Anzeigner 110 (82) 32–33.

[5] K.J. Lee, T.M. Lee, and M.Y. Yang, 2007, Tool wear monitoring system for CNC end milling using a hybrid approach to cutting force regulation, International Journal Advance Manufacturing Technology, 32:8-17.

[6] S. Braun, E. Lenz, C.L. Wu, 1982, Signature analysis applied to drilling, Journal Mechanical Design, Transactions of the ASME, 104: 268–276.

[7] S.C. Lin, C.J. Ting, 1995, Tool wear monitoring in drilling using force signals, Wear 180 (1-2) 53–60.

[8] E. Jantunen, H. Jokinen, 1996, Automated On-line Diagnosis of Cutting Tool Condition (Second version), International Journal of Flexible Automation and Integrated Manufacturing 4 (3-4) 273–287.

[9] Y.-C. Chang, K.-T. Lee, and H.-Y. Chuang, 1995, Cutting force estimation of spindle motor, J. Contr. Syst. Technol., 3/2:145-152.

[10] X. Li, 2005, Development of current sensor for cutting force measurement in turning, IEEE Transactions on Instrumentation and Measurement, 54(1):289-296.

[11] A. Noori-Khajavi, 1992, Frequency and time domain analyses of sensor signals in a drilling process and their correlation with drill wear, PhD Thesis, Oklahoma State University, Stillwater, OK.

[12] K. Patra, S.K. Pal, and K. Bhattacharyya, 2007, Artificial neural network based prediction of drill flank wear from motor current signals, Applied Soft Computing, 7:929-935.

[13] R.F. Hamade, C.Y. Seif, and F. Ismail, 2006, Extracting cutting force coefficients from drilling experiments, International Journal of Machine Tools & Manufacture, 46:387-396

[14] S.E. Oraby and D.R. Hayhurst, 2004, Tool life determination based on the measurement of wear and tool force ratio variation, International Journal of Machine Tools & Manufacture, 44:1261-1269.